



	Experiment title: Magnetism of mass-selected FeRh B2 nanocrystals in epitaxy on perovskite oxide	Experiment number: HC-5210
Beamline: ID12	Date of experiment: from: 10 May 2023 to: 15 May 2023	Date of report: 7 June 2023
Shifts: 18	Local contact(s): Fabrice WILHELM	<i>Received at ESRF:</i>
Names and affiliations of applicants (* indicates experimentalists): Main proposer: DUPUIS Véronique* (Laboratory UCB Lyon 1 - CNRS UMR 5306 Institut Lumière Matière (iLM) Domaine scientifique de La Doua, 6 rue Ada Byron FR – 69622 VILLEURBANNE Cedex) Co-Proposers and experimentalists: MOREAU Joseph* (iLM), BUGNET Matthieu* (MATEIS) and GONZALES Sara*(INL),		

Report:

Scientific background :

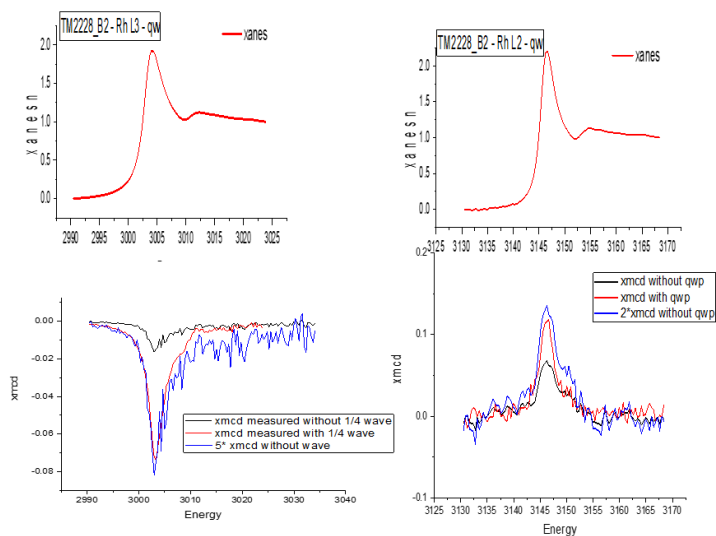
Near equiatomic composition, FeRh bulk alloys exhibit a CsCl-type (B2) chemically ordered phase related to a metamagnetic transition from an antiferromagnetic (AFM) to a ferromagnetic (FM) state close to ambient. Recently, we underlined the main role of Rh atoms on the metamagnetic transition for samples with high-density FeRh nanoparticles assemblies, where rhodium kept a residual FM signature even at low temperature due to strong iron coupling^[1]. The objective of this present proposal is to study **low-density samples**, of mass-selected FeRh nanoparticles (NPs) **grown on perovskite oxide, from X-ray absorption spectroscopy and magnetic circular dichroism (XAS/XMCD) experiments at Rh L-edges on ID12 beamline to explore interfacial strain effects on the magnetic order of epitaxial FeRh nanoparticles.** Such inquiries would require both the use of quarter-wave plate (qwp) to enhance the circular polarization rate and a Silicon Drift Detector (SDD) with appropriate energy filter mounted in the 8T-cryomagnet to improve the signal to noise ratio of XAS/XMCD of such diluted hybrid-nanostructures.

Sample preparation and Characterization

FeRh clusters were produced in gas phase with two different diameters 3 and 7 nm by Mass-Selected Low Energy Cluster Beam Deposition (MS-LECBD) in UHV chamber on Si, SrTiO₃ (STO) and Nb doped STO (Nb-STO) substrates at Lyon with a carbon capping before their transfer in air. We have verified that as-prepared NPs are in the chemically disordered fcc A1 phase, while UHV post-annealing above 600°C leads systematically to chemical ordering for FeRh nanocrystal towards the B2 phase^[2]. Notice that we also evidences epitaxy relationship for our annealed FeRh clusters deposited on STO and Nb-STO substrates^[3] while XAS/XMCD surface sensitive signal at L_{2,3} Fe edge revealed strong FM signature at any temperature for sample on Si substrate but with additional oxidized contribution on both STO and Nb-STO substrates which can be reduced by *in situ* annealing in the DEIMOS UHV chamber at SOLEIL.

Experimental results

By using two Silicon Drift detectors (SDD) mounted in the vacuum 8T-cryomagnet chamber, we first measured 140nm-thick FeRh on Si substrate annealed 3h 700°C (TM2228-B2) sample as a reference to optimize the X-ray beam alignment on a 10° sample holder at room temperature under 2T applied magnetic field and in order to estimate the circular polarization enhancement obtained by using or not the qwp. In both cases, a clear XANES



signature characteristic of the chemically ordered B2 FeRh phase has been evidenced on this sample from oscillation just after the white Rh $L_{3,2}$ edges^[4]. While the XMCD signal at the Rh L_3 (resp. at L_2) edge has been multiplied by 5 (resp. by 2) by comparing without and with qwp, the polarization rate has been found to increase at the Rh L_3 (L_2) edge from 5% (resp. 12%) to 25 % (resp. 24%) (as seen in Fluorescence mode in Fig. 1).

Fig. 1 XANES at the Rh $L_{3,2}$ -edges (Top) on annealed 140nm-thick FeRh NPs on Si with C-capping (TM2228-B2) sample reference and the XMCD comparison signal (Bottom) with (in red) and without (in blue) qwp.

Then the following thin samples with a few nm of equivalent FeRh thickness were measured two by two in 10° grazing incidence with the qwp by using SDD detectors. Note that the samples can only stick with carbon tape on the 10° sample holder for room temperature measurements while they have to be silver pasted for higher temperature measurements up to 420K. By optimizing couple of samples, we have been able to alternate XAS/XMCD measurements and long annealings in an additional furnace. During the run beamtime, we have been successful in measuring 3 samples already annealed and 3 before and after annealing from 530°C to 580°C .

Here, we report comparative XAS/XMCD results at 2T and one hysteresis loop at L_3 -Rh edge up to 7T:

- **Thin FeRh NPs with 7 nm in diameter on Si** with C-capping (equivalent FeRh thickness of 3 nm) TM2219 sample (as-prepared and annealed 3h at 530°C + 1h at 580°C) to compare to reference TM2228 B2.
- **Thin FeRh NPs with 7 nm in diam. on Nb-STO** with C-capping (equivalent FeRh thickness of 1 nm) TM2335 (as-prepared sample and annealed 3h at 530°C) to compare to above sample TM2219 on Si substrate.
- **Thin FeRh NPs with 3 nm in diameter on Nb-STO** with C-capping (eq. FeRh thickness of 0.5 nm) TM2334 (as-prepared sample and annealed 3h at 530°C + 1h at 580°C) to compare with 2 already annealed samples on STO TM2109 (at 600°C) and TM2127 (at 800°C).

First of all, for in place annealing temperature $T \leq 530^\circ\text{C}$, we noted nor clear structural, nor magnetic evolution from XANES/XMCD spectra at L-Rh edge (as seen in Fig. 2 for a fixed 7nm FeRh NPs size regardless of the type of substrate : Si or Nb-STO).

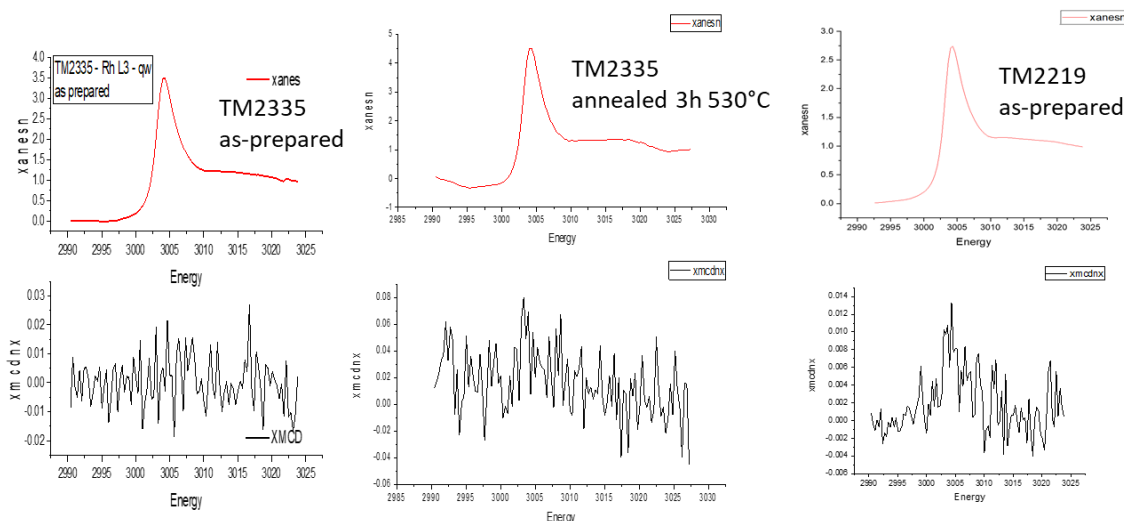


Fig. 2: No clear XANES/XMCD evolution at Rh- L_3 edge at 300 K and 2T obtained on FeRh NPs with 7 nm in diameter TM2335 (as-prepared sample and annealed at 530°C) on Nb-STO compared to TM2219 (as-prepared) on Si substrate.

Above a critical annealing temperature, we systematically obtained metallic XANES/XMCD evolution at the Rh- $L_{2,3}$ edges at 300K and under 2T, leading for annealed samples to similar tendency as for the reference thick (TM2228 B2) annealed sample. Indeed, we clearly identify by XANES at Rh-L edge a structural change from A1 fcc chemically disordered for as-prepared sample to B2 CsCl chemically ordered FeRh upon vacuum annealing at $T > 580^\circ\text{C}$, accompanying with XMCD change from paramagnetic to ferromagnetic order transition (as seen in Fig. 3 for FeRh NPs with 7 nm in diameter deposited on Si and in Fig. 4 for FeRh NPs with 3 nm in diameter on STO based substrate with C-capping).

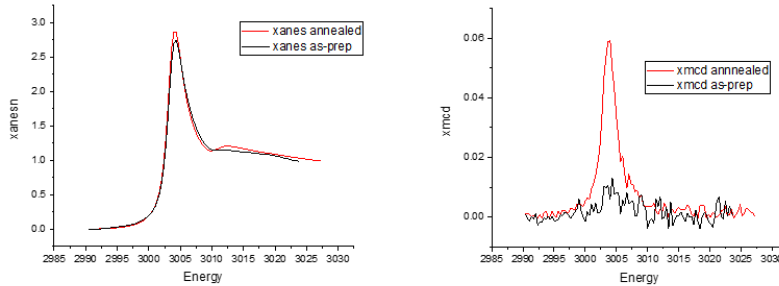


Fig. 2: XANES/XMCD 300 K and 2T at the Rh L_3 -edges on TM2219 sample on Si substrate (7 nm in diameter FeRh NPs) as-prepared (in black) and annealed : 3h at 530°C + 1h at 580°C (in red)

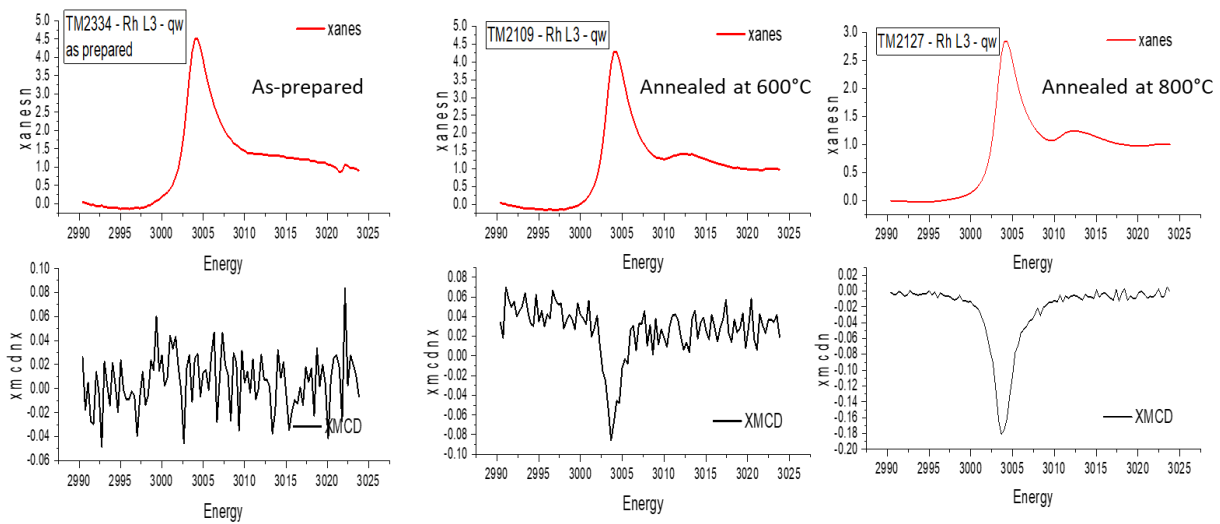


Fig. 3: XANES/XMCD signal evolution at Rh- L_3 edge at 300 K and 2T obtained on FeRh NPs with 3 nm in diameter on STO based substrate with C-capping (eq. FeRh thickness of 0.5 nm): TM2334 (as-prepared sample) on Nb-STO, TM2109 (annealed at 600°C) and TM2127 (annealed at 800°C) on STO showing the progressive A1 \rightarrow B2 (in red XANES curves) / PM \rightarrow FM (in black XMCD curves) transition as a function of UHV annealing temperature.

As a conclusion, this present XAS/XMCD study at Rh $L_{2,3}$ edges on very diluted FeRh NPs samples clearly underlines the fact that SDD with appropriate energy filter adapted in the 8T-cryomagnet improve the signal to noise ratio and that the use of qwp enhance the circular polarization rate enough to be able to detect structural and induced magnetic moment at the local Rh environment for FeRh NPs assemblies with less than a few nm of equivalent FeRh thickness^[1]. But reversely to our previously study on thick FeRh nanogranular sample (with diameter greater than 30 nm), no metamagnetic AFM/FM transition have been detected on well-separated B2 FeRh NPs (with diameter lower than 10 nm) from XMCD signal at the Rh L_3 -edge in the range of temperature 300-420 K regardless applied magnetic field 2-7 T, thermal treatments and strain from epitaxy on oxide perovskite substrates. This study have revealed similar magnetic behaviour for strongly correlated Fe and Rh atoms in well-defined B2 FeRh nanoalloys which confirm the main role of finite size effect in metamagnetic transition.

REFERENCES

- ¹ See our experimental report HC-4794 on ID12 beamline
- ² A. Hillion et al. Phys. Rev. Lett. 110, 087207 (2013) and G. Herrera et al. EPJAP 97, 32 (2022)
- ³ See our experimental report A32-3-745 on BM32 beamline
- ⁴ A. Aubert, K. Skokov, G. Gomez, A. Chirkova, I. Radulov, F. Wilhelm, A. Rogalev et al. IEEE Trans. Mag. 71, 6002409 (2022)